Experimental Study of Three-Lifting-Surface Configuration

C. Ostowari* and D. Naik†
Texas A&M University, College Station, Texas

The aerodynamic ramifications of utilizing three lifting surfaces as opposed to the conventional or canard lifting configurations have been studied on a theoretical basis by previous researchers. This paper presents an experimental investigation of various configuration modifications for an unyawed typical business jet at a Reynolds number of 1.3 × 10⁶. In general, the data are untrimmed. The three-surface lift is marginally different from the conventional and has lower slope and maximum lift coefficient than the canard configuration. A decrease in gap adversely affects the pitching moment characteristics. A smaller stagger leads to better aerodynamic and stability characteristics, except that the lift-dependent drag might increase. A decrease in span of the forward wing has minimal effect on the lift and drag. A variation in the incidence angles of either or both the forward and aft wings changes the zero-lift moments of the configuration, while marginally affecting overall lift and drag.

Nomenclature

a.c. = aerodynamic center
AR = aspect ratio, b^2/S
b = lifting surface span
c = lifting surface mean aerodynamic chord
C_D = drag coefficient, drag/qS
C_L = lift coefficient, lift/qS
C_m = pitching moment coefficient w.r.t. $0.25c_w$, moment/qSc_w
f.w. = forward wing (canard)
g = gap (vertical distance between the a.c. of wings), distance/c_w
L = fuselage length
q = freestream dynamic pressure
RN = Reynolds number w.r.t. c_w
s = stagger (horizontal distance between the a.c. of wings), distance/c_w
S = lifting surface exposed planform area
TLC = three-lifting-surface configuration
α = angle of attack
δ = incidence angle
Δ = difference
λ = taper ratio
Λ = sweep angle at $0.25c$

Subscripts

c = canard (forward wing)
t = tail (aft wing)
w = main wing
0 = zero-lift condition

Introduction

THE theories and modifications to the theories of Prandtl and Munk have been used by a number of researchers[1-5] to explore the minimum induced drag of multiplanes (aircraft with multiple wings). These studies have yielded comparative predictions of the induced drag and static longitudinal stability of conventional aircraft, canard, and three-surface configurations. The effect of variations in gap and stagger are also an integral portion of these studies.

Kendall[6-8] has summarized these analytical results, theorizing that minimum induced drag should be attainable at any c.g. location so long as equal and opposite vertical loads are applied by the forward and aft lifting (or trimming) surfaces. Furthermore, these minimum induced drag loads should be achievable at any useable c.g. location, within the practical limits set by the size and shape of the lifting surfaces.

An important and pragmatic concern about these theoretical studies is that idealizing assumptions have been made, usually closely allied to Prandtl's and Munk's assumption of an elliptical spanwise lift distribution. Both Butler[3] and Kroo[4] have suggested that for nonelliptical lift distributions with pure canards, the effects are significantly different from results deduced using purely elliptical distributions. Butler predicts that the three-surface induced drag at both typical cruise and high-lift conditions is lower than the induced drag of either a conventional aircraft or a canard-wing type.

A recent analytical study, by Selberg and Rokhsaz,[9] of the aerodynamic tradeoff between the three configurations shows that the three-surface one is superior to the canard only at lower stabilator aspect ratios and that the overall induced drag penalty is not sufficiently different to be of primary concern in the configuration selection process.

The conventional airplane configuration has been the subject of numerous experimental investigations. Wind-tunnel measurements of wing-canard interference[10] have shown potential advantages, in terms of aerodynamic efficiency, high-lift capability and stall characteristics, for the lower subsonic speed range. Other experimental studies[11] have shown the importance of proper canard airfoil selection to the longitudinal stability of canard-wing configurations. These studies have also pointed out the need for basic experimental data on a typical three-lifting-surface configuration.

This paper presents aerodynamic force and moment measurements from a series of wind-tunnel experiments using a practical airplane configuration to ascertain how nonelliptical lift distributions affect the lift, drag, and static longitudinal stability for a three-surface configuration. The configuration selected for the research was similar to a current tail-aft business jet aircraft that is modified by the addition of a forward wing and fuselage extension for stagger.

Comparisons are made between the conventional (tail-aft), canard, and three-surface configurations. The effect of variation in tail and forward wing incidence angles and the effects of stagger and gap are also studied.

Procedure

The wind-tunnel testing was carried out, on a 0.15 scale model of a typical business jet, at the Texas A&M University

Received June 22, 1986; revision received May 25, 1987.

*Associate Professor, Aerospace Engineering Department. Member AIAA.

†Graduate Research Assistant, Aerospace Engineering Department. Student Member AIAA.

2.13 × 3.05 m low-speed wind tunnel. The tunnel and its six-component, pyramidal, virtual center, external balance is described in Ref. 12. The model has a removable fuselage extension to allow for two different stagger values. Two forward wing spans were studied. The larger forward wing had the same span as the horizontal tail, while the smaller forward wing had a span which was 75% of the horizontal tail span. The location of the forward wing is shown in Fig. 1. The circumferential band just forward of the main wing indicates where the fuselage can be split to include the fuselage extension plug.

Provisions were made to allow for forward wing and horizontal tail incidence variation. The effect of gap variation was studied by placing the horizontal tail at two different locations on the vertical tail. The various model configurations are shown schematically in Fig. 2 and tabulated in Table 1.

Of the 98 possible configurations, 66 were studied and selected results are presented here. Pertinent model dimensions are given in Table 2.

All force and moment measurements were made on an unyawed model at a dynamic pressure of 2.16 kPa (45 lb/ft^2), which corresponds to a Reynolds number, with respect to a mean aerodynamic chord of 0.3048 m (1 ft), of 1.3×10^6. The angle-of-attack range studied was −8 to 20 deg in increments of 2 deg. All data were corrected for tunnel wall effects (wake blockage, solid blockage, buoyancy drag, etc.) using the standard procedure given in Ref. 13. Although dimensional quantities are given here in SI units, measurements were made in U.S. customary units. Unless specifically stated, all force and moment data are nondimensionalized w.r.t. S_w.

During testing, the force and moment data were referred to the quarter-chord location of the mean aerodynamic chord of the model main wing. Data for C_m, referred to $0.25c_w$, vs C_L is studied to compare values at the zero-lift condition and to compare neutral points. The C_{m0} values are independent of the c.g. location and the pitching moment slopes are used to estimate the neutral points for the various configurations. These data can also be used to compare the pitching moment characteristics for various configurations at the same static margin by simple rotations about the zero-lift points.[14] The data are not trimmed at a fixed stability level. The discussion in the following section should be tempered by this fact.

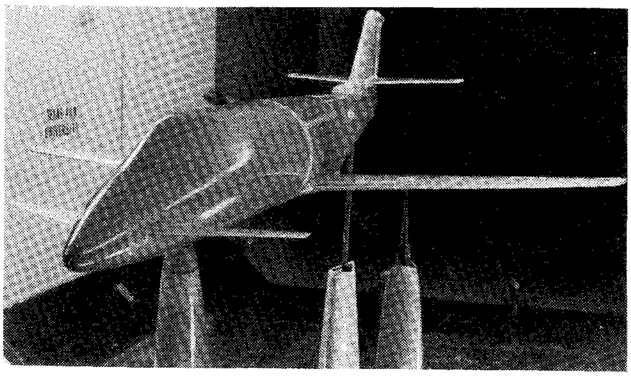

Fig. 1 Three-lifting-surface model.

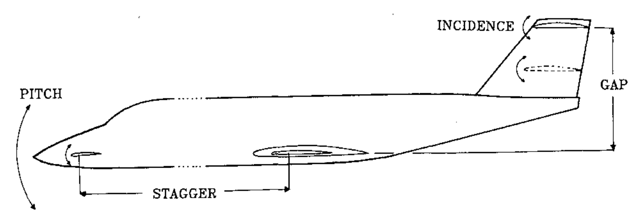

Fig. 2 Model configurations.

Results

The reduced data are presented here in the form of plots of lift coefficient vs angle of attack, drag coefficient vs lift coefficient, and pitching moment coefficient vs lift coefficient. It is important to note that all the plotted data are reduced w.r.t. S_w. For clarity, pertinent tables are superimposed on some of the plots. These tables contain both data reduced w.r.t. S_w and data reduced w.r.t. the total planform area. Omissions (i.e., data w.r.t. total planform area not presented here, because of space restrictions) can easily be deduced from the plotted data and the information contained in Table 2. Furthermore, in the interests of more clarity and less clutter, only selected drag data points have connecting lines passing through them.

Comparison between TLC and Conventional Configuration

Figure 3 shows a comparison between the conventional configuration and the TLC. The characteristics are for an unstretched aircraft with a high tail at a δ of −2 deg, with and without a large forward wing that can be set at three different incidence angles. The configurations have common fuselage, main wing, and vertical tail.

Table 1 Model configurations

Configuration	Variables
Wing + fuselage	2 fuselage sizes
Wing + fuselage + horizontal tail	2 fuselage sizes 2 tail positions 3 tail incidence angles
Wing + fuselage + forward wing	2 fuselage sizes 2 forward wing sizes 3 forward wing incidence angles
Wing + fuselage + forward wing + horizontal tail	2 fuselage sizes 2 forward wing sizes 2 tail positions 3 forward wing incidence angles 3 tail incidence angles

Table 2 Pertinent model dimensions[a–c]

b_w	2.00 m
b_t	0.336 b_w
b_c	large = 0.336 b_w, small = 0.257 b_w
c_w	0.3048 m
c_t	0.574 c_w
c_c	large = 0.465 c_w, small = 0.338 c_w
S_w	0.5529 m^2
S_t	0.204 S_w
S_c	large = 0.081 S_w, small = 0.047 S_w
AR_w	7.2
AR_t	4
AR_c	large = 5.3, small = 5.3
$g_{w,t}$	1.64 c_w and 0.8 c_w
$s_{w,c}$	4.69 c_w and 3.46 c_w
L	extended = 9.50 c_w, original = 8.27 c_w
λ_w	0.403
λ_t	0.469
λ_c	large = 0.386, small = 0.386
Λ_w	12.7 deg
Λ_t	25 deg
Λ_c	large = 30 deg, small = 30 deg

[a]Main wing section: modified NACA 64A109; other wings: NACA 64A008. [b]Main wing dihedral: 2.5 deg; other wings: no dihedral. [c]All wings untwisted.

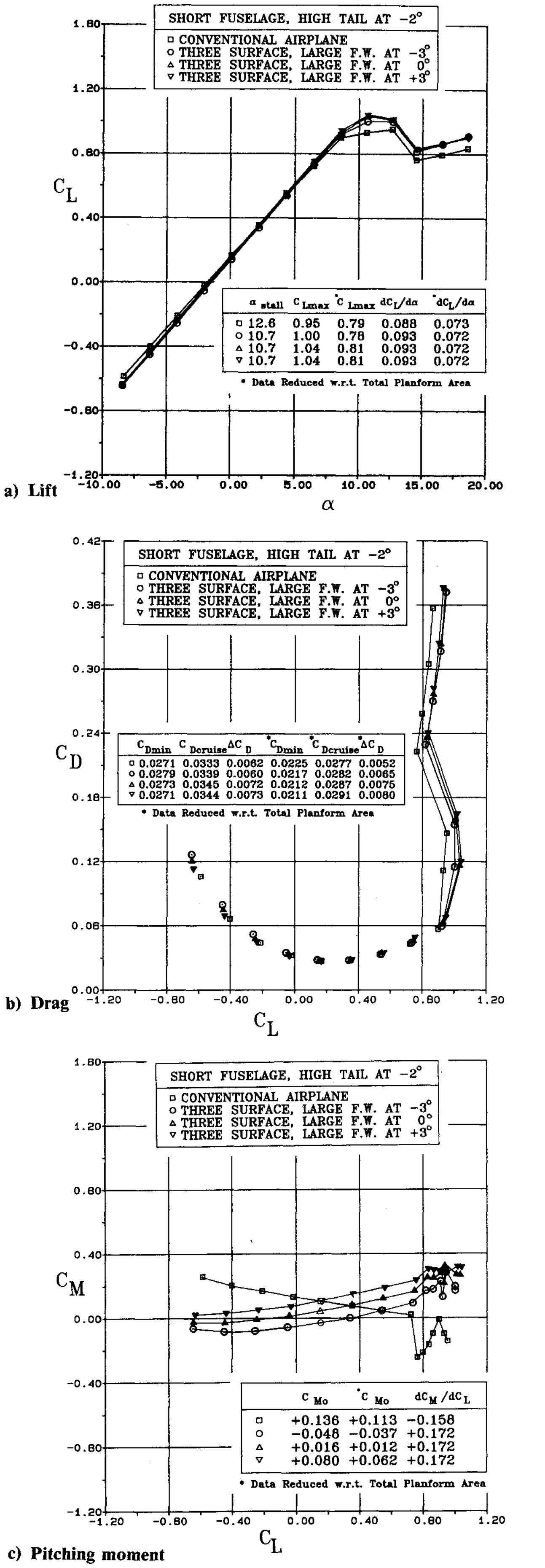

Fig. 3 Comparison between the three-surface and conventional configurations and the effect of forward wing incidence.

The lift curve slope and maximum lift, w.r.t. S_w, are higher for the TLC, indicating the extra lift obtained from the forward wing. This does not, however, imply that the forward wing has a favorable effect on the flow over the main wing, a possibility, mentioned by Feistel et al.,[10] for canard-wing combinations. The data-reduced w.r.t. total planform area show the marginal degradation in the slope and marginal improvement in maximum lift coefficient with the addition of the third lifting surface.

For subsonic aircraft, the gap $g_{w,c}$ is an important determinant[10] of the main wing performance. However, in the present study, this gap effect was not studied. The variation in $g_{w,t}$ is presented in a later subsection.

The balance resolution for drag coefficient is ± 0.0002. For the lift coefficient range of -0.2 to 0.8, including values in and around typical cruise (chosen as $C_L = 0.55$ here), the TLC has higher total drag (w.r.t. S_w) and higher drag coefficient (w.r.t. total planform area). With the assumption that there is minimal separation and, consequently, negligible pressure drag at cruise, the difference ΔC_D between the drag at some lift coefficient and the minimum drag can be said to give some indication of the lift-dependent drag. These values (Fig. 3b) indicate that, at cruise, the TLC induced drag is probably greater than the conventional induced drag. However, this result is marginally useful as none of the configurations were trimmed at cruise.

Figure 3b shows the marginal drag benefit at high (>0.8) lift coefficients for the TLC over the conventional. The results seem in agreement with Butler's theoretical predictions regarding the lower drag at high-lift conditions.[3] However, the configurations have nonlinear pitching moment characteristics (Fig. 3c) for C_L greater than 0.75. The fair amount of control of surface deflection required for trim would again adversely affect the drag and thus could nullify any possibility of a drag benefit.

The pitching moment plots show the neutral point for the conventional aircraft to be $0.158c_w$ aft of the quarter-chord reference point and to move forward to $0.172c_w$ with the addition of the forward wing. As mentioned earlier, the moment curves may be rotated about their C_{m0} values for comparisons at the same static margin. The zero-lift pitching moment is highest for the conventional. For the TLC to fly in trim with the same, arbitrarily chosen static margin and at the same design lift coefficient as the conventional, it would require considerable control surface deflection, which would adversely affect the drag.

At high-lift conditions, the pitching moment characteristics are nonlinear. The amplitudes of the fluctuations in pitching moment are smaller for the TLC, at all three incidence angles, than the amplitude of the fluctuations for the conventional airplane. However, the conventional is seen to pitch down at stall.

Effect of Variation in Forward Wing Incidence Angle

Figure 3 also shows the effect of variation in forward wing incidence angle. This variation has a minimal effect on the TLC lift, reflected in the $C_{L\max}$, near stall. There is a marginal improvement in the high-lift drag characteristics with an increase in forward wing incidence angle. The variation in incidence does not affect the neutral point of the TLC. As would be expected, C_{m0} increases with an increase in forward wing incidence angle.

Comparison between TLC and Canard Configuration

Figure 4 compares the characteristics of basically the same TLC as in the previous subsection with the canard configuration. These configurations have a common fuselage and vertical tail. The forward wing incidence angle is fixed at 3 deg. The δ for the horizontal tail is -2 deg. The horizontal tail can be moved to provide the two different gaps shown in Fig. 2. This gap effect is discussed in the next subsection.

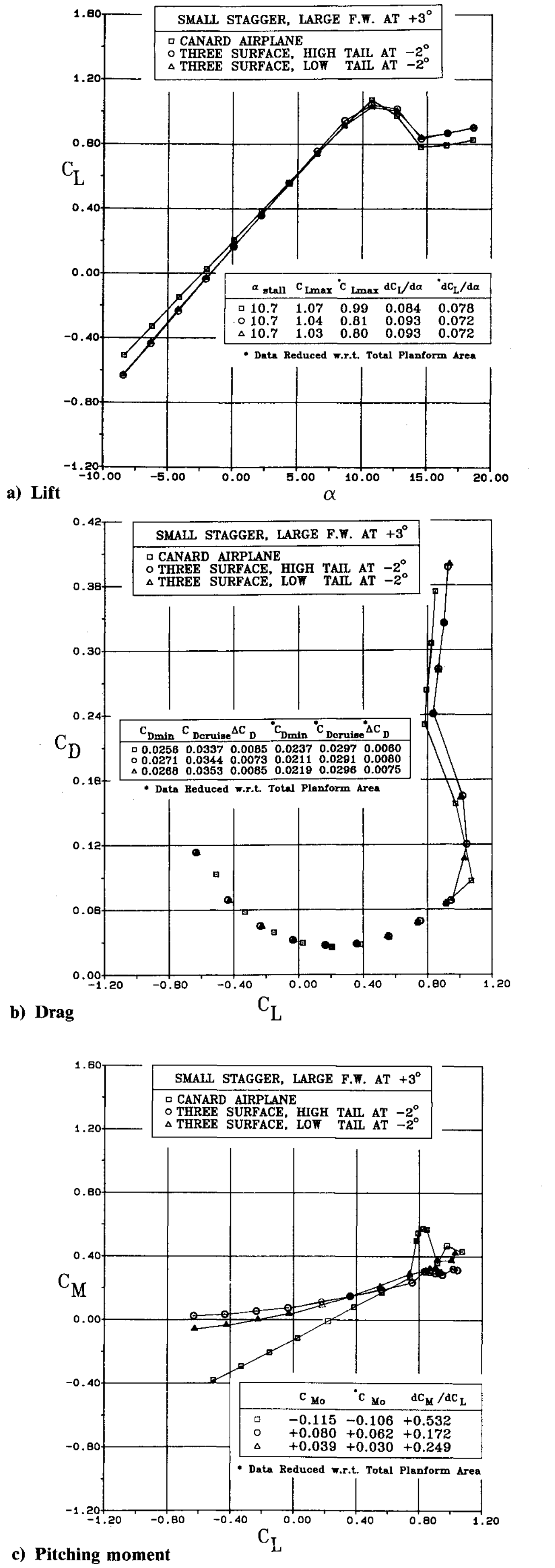

Fig. 4 Comparison between the three-surface and canard configurations and the effect of gap $g_{w,t}$.

For data reduced relative to total planform area, the canard configuration has a far higher maximum lift and an 8% higher slope (see Fig. 4a). The stalling angle of attack is the same.

The canard has lower minimum drag (Fig. 4b) but a higher minimum drag coefficient, w.r.t. total planform area. The fact that the canard has fewer interfering surfaces probably does not contribute to this difference, as the next subsection shows the minimal effect of gap $g_{w,t}$ on the aerodynamic characteristics. At a typical cruise lift coefficient, the starred ΔC_D indicate that the TLC-induced drag is probably more than the canard-induced drag. However, this may be viewed in the perspective of Selberg and Rokhsaz's finding,[9] for trimmed configurations, that there is an overall induced drag benefit with a TLC that may not be sufficient to be of primary concern in the configuration selection process.

The pitching moment in Fig. 4c shows the negative zero-lift moment for the canard. As would be expected, the neutral point for the canard is much further ahead, $0.532c_w$ in front of $0.25c_w$, than those for the TLC. The canard would require considerable control surface deflection for trim at typical cruise, again adversely affecting the drag. The TLC probably would be easier to control at the high C_L conditions, as evidenced by the smaller fluctuations in pitching moment.

Effect of Variation in Gap

The importance of the forward gap $g_{w,c}$ has been discussed by other authors[10] in connection with canard configurations. This subsection deals with the effect of variation in $g_{w,t}$ for a TLC with $g_{w,c}$ close to zero. Although, for the sake of brevity, the conventional configuration data are not presented, it is important to note that the variation in $g_{w,t}$ has a significant effect on the aerodynamic characteristics of the conventional configuration. The high-tail conventional lift is higher and the drag is less than the low-tail conventional.

The gap $g_{w,t}$, has minimal effect on the TLC lift curve (Fig. 4a). The maximum lift coefficient, lift curve slope, and stalling angle of attack do not change appreciably with gap. The drag characteristics (Fig. 4b) are largely, except for a small decrease in ΔC_D around cruise, unaffected by the decrease in gap. The change in the lift-dependent drag indicates that the gap has a small effect on this drag. The minimal effect of the change in gap on the overall lift and drag characteristics of the TLC, could imply that the forward and main wing wakes are probably well below the lowest horizontal tail position. Since the gap has a significant effect on the conventional configuration, the forward wing of the TLC probably has some favorable effect on the flow over the main wing.

Most of the current TLC literature gives some consideration to the variation in gap between the main wing and the aft wing. The minimal effect of the gap shown here could possibly lead to simplifying assumptions, regarding the aft gap, for future theoretical models. On the other hand, it could be purely coincidental.

The C_m curves (Fig. 4c) show positive C_{m0} decreasing with a decrease in gap. The neutral point for the high tail is $0.172c_w$ ahead of the quarter-chord point. For the low tail it is $0.249c_w$ ahead. The low tail will require more control surface deflection for trim at the chosen cruise C_L of 0.55. In both cases, the curves are somewhat nonlinear in the high C_L range. Since the overall lift and drag are largely unaffected by the change in gap, the difference in the pitching moment characteristics probably arises purely from the different moment arms, provided by the different gaps, for the drag of the aft lifting surface.

Effect of Variation in Stagger

The effect of a change in stagger $s_{w,c}$ between the forward and main wing of the TLC is shown in Fig. 5. The values for the two staggers were given earlier in Table 2. The configuration has a high tail and a large forward wing set at an incidence angle of 3 deg. Results are shown for tail incidence angles of −2 and −4 deg. The effect of the variation in tail incidence angle is discussed in the next subsection.

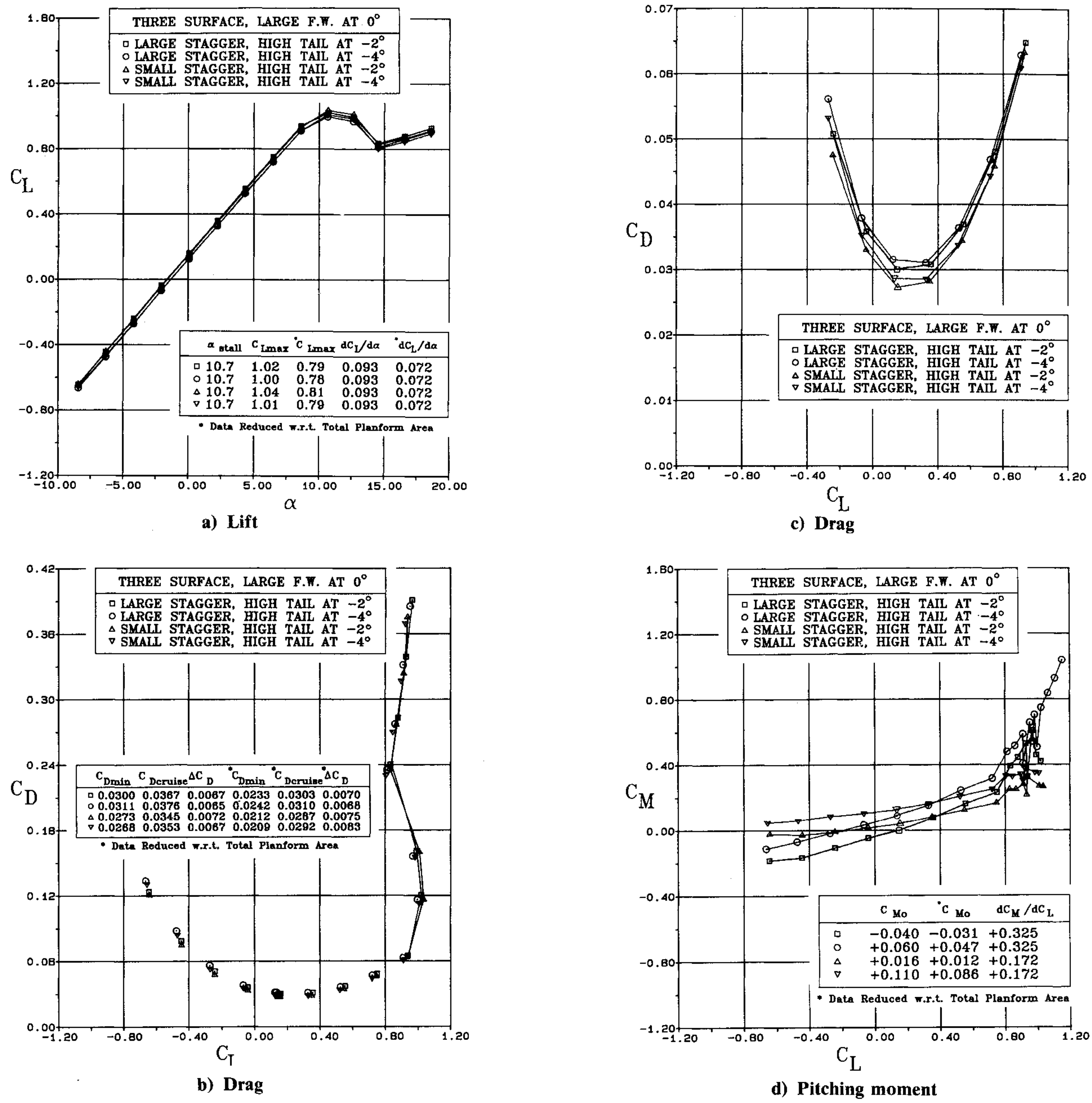

Fig. 5 Effect of stagger and the effect of tail incidence.

Figure 5a shows the relatively small effect of this change in stagger on the lift characteristics. The stalling angle of attack and lift curve slope are unchanged. There is a less than 2% decrease in the $C_{L\max}$ in going from the smaller to the larger stagger.

The effect on drag is minimal in the high-lift regions (Fig. 5b). The overall drag in and around cruise is understandably higher for the stretched version because of the larger fuselage wetted area available. However, if the ΔC_D values are a fair indication, the lift-dependent drag at cruise increases with this decrease in stagger. The drag polars in and around cruise are shown on a larger scale in Fig. 5c for clarity.

The pitching moment, w.r.t. $0.25c_w$, in Fig. 5d is seen to have an increase in zero-lift moment with this decrease in stagger. Further, the neutral point for the larger stagger is roughly $0.15c_w$ ahead of the neutral point for the smaller stagger. The pitching moment curves for the larger stagger have larger fluctuations in the high-lift region. Incidentally, from nonaerodynamic criteria (i.e., a simple weight balance), one would expect the c.g. of the longer body to be $0.095c_w$ ahead of the c.g. for the shorter body. This distance is small because the fuselage plug is inserted close to the original c.g.

Effect of Variation in Tail Incidence Angle

This effect is partially presented in Fig. 5. Although for clarity, all three tail incidence angles were not simultaneously presented in the coefficient plots, the effect of variation in tail incidence angle merits some discussion. Further, it should be noted that the following discourse is confined to high-tail configurations. Low-tail inferences can be made from a synthesis of this subsection with the effect of gap presented earlier.

A variation in the incidence angle of the horizontal tail marginally affects the lift and drag. The stalling angle of attack and lift curve slope do not change with tail incidence angle for all the configurations studied. Also, there is a marginal decrease in $C_{L\max}$ and an increase in $C_{D\min}$, when the tail incidence angle is decreased from 0 to -4 deg. For example, for the conventional configuration, the $C_{L\max}$ decrease is 5% and the $C_{D\min}$ increase is 20 counts. There is an overall increase in lift with increasing incidence angle and there is a 1 deg range for the angles of attack at which zero lift occurs for the three tail incidence angles. There is a slight improvement in high-lift drag with an increase in tail incidence angle. The basic pitching moment characteristics remain the same but, as expected,

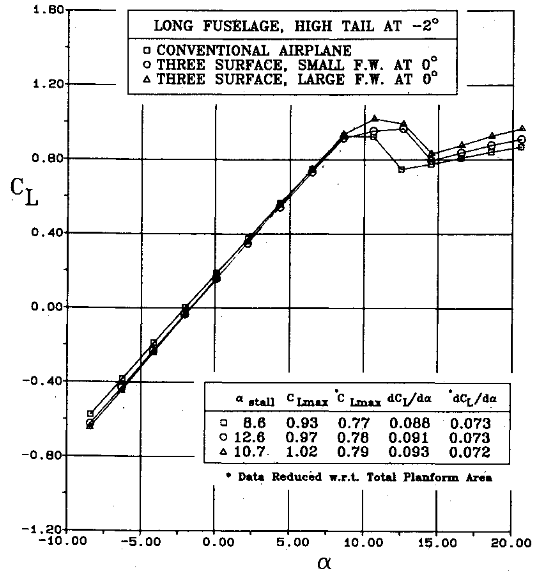

a) Lift

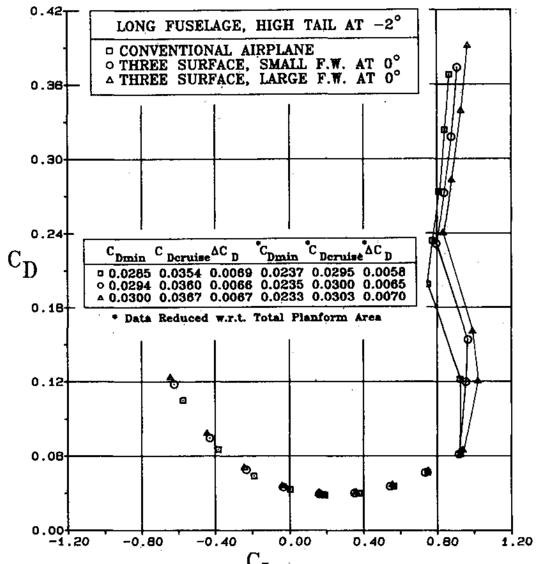

b) Drag

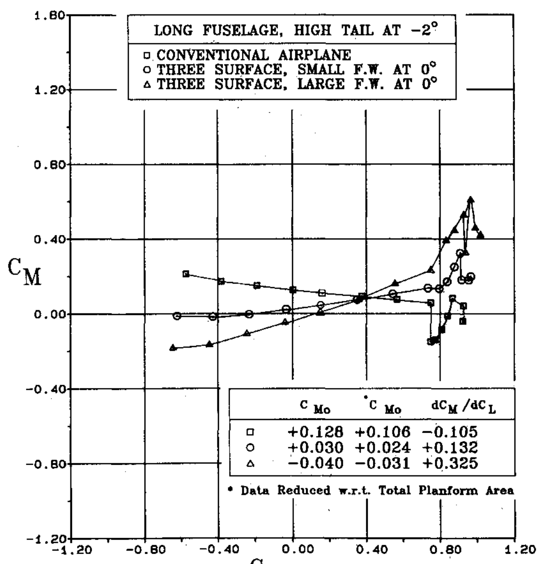

c) Pitching moment

Fig. 6 Effect of forward wing span.

the zero-lift pitching moment increases with a decrease in tail incidence angle.

Effect of Variation in Forward Wing Span

In the previous subsections, results have been presented for a TLC with a forward wing whose span is the same as that of the horizontal tail. Figure 6 shows a comparison between the aerodynamic characteristics of a stretched TLC with a forward wing of span $1.00b_t$ and those of a stretched TLC with a forward wing of span $0.75b_t$. In both cases, the forward wing is at an incidence angle of 3 deg and the gap $g_{w,c}$ and stagger $s_{w,c}$ are not changed. The tail is high and at an incidence angle of -2 deg. The data for a conventional airplane (identical except that it lacks the forward wing) have been superimposed for comparison.

There is no noticeable change in the lift characteristic (when it is reduced relative to total planform area) of the TLC with an increase in the forward wing size. The stalling angle of attack, lift curve slope, and maximum lift coefficient are all basically unaffected by the change in forward wing size. In and around cruise (Fig. 6b), the TLC with the large forward wing has slightly higher total drag, probably because of larger wetted surface area. The ΔC_D shows a small change with span, probably implying marginal change in the lift-dependent drag.

The pitching moment data in Fig. 6c shows that the zero-lift moment decreases with forward wing size and is negative for the large span. The neutral point moves forward roughly 20% with an increase in span.

Conclusions

A series of wind-tunnel experiments have been carried out to investigate the aerodynamic characteristics for a three-lifting-surface configuration. Comparative data between the three-surface, canard, and conventional configurations, with identical fuselage, main wing, and vertical tail, are also superimposed where appropriate. Wherever possible, parallel data reduced w.r.t. the total planform area are given for comparison with the data reduced w.r.t. a standard planform area (the main wing). In general, the data are for an untrimmed aircraft.

Lift

The three-surface lift is marginally different from the conventional and is lower (in slope, maximum lift) than the corresponding canard configuration. The overall characteristic (slope and maximum lift) improves with an increase of the incidence angle of either the forward or aft lifting surfaces. It is basically unaffected by a decrease in the size of the forward wing. There is no change with a variation in the aft wing to main wing gap.

Drag at Cruise

The three-surface drag in and around cruise is greater than the drag of the conventional and comparable to the canard configuration. Drag increases with an increase in forward wing incidence angle, decrease in aft wing incidence angle, increase in forward to main wing stagger, and decrease in aft to main wing gap. There is a slight increase with an increase in forward wing size.

Drag at High-Lift Conditions

There is no change with a change in the aft to main wing gap. There are slight drag benefits with an increase in forward wing incidence angle and an increase in aft wing incidence angle.

Zero-Lift Moment

In order to have desirable pitching moment characteristics, the three-surface and canard configurations will require considerable control surface deflection, adversely affecting the drag. The three-surface zero-lift moment can be set to a desired value by realigning the surfaces. For example, it increases with an increase in the forward wing incidence angle, decrease in aft wing incidence angle, increase in aft to main wing gap, decrease in stagger between the forward and main wing, and decrease in the forward wing span.

Neutral Point

As would be expected, the three-surface neutral point is between the conventional and canard neutral points. It does not change with a change in either forward or aft lifting surface incidence angle. The neutral point moves forward with a decrease in aft to main wing gap, an increase in forward to main wing stagger, and an increase in forward wing span.

Acknowledgements

This research was supported by NASA Langley through Grant NAG(1)-344, with contract monitor Mr J. Stickle. The authors wish to thank Messrs. D. Howe and E. Kendall for their help and suggestions. The models were supplied by Gates Learjet Corporation which also covered all model modification and transportation expenses.

References

[1]Naylor, C. H., "Notes on the Induced Drag of a Wing-Tail Combination," Aeronautical Research Committee, London, R&M 2528, 1954.

[2]Laitone, E. V., "Prandtl's Biplane Theory Applied to Canard and Tandem Aircraft," *Journal of Aircraft*, Vol. 17, April 1980, pp. 233–237.

[3]Butler, G. F., "An Analytical Study of the Induced Drag of Canard-Wing-Tail Aircraft Configurations with Various Levels of Static Stability," Royal Aircraft Establishment, London, Tech. Rept. 81052, 1981.

[4]Kroo, I. M., "Minimum Induced Drag of Canard Configurations," *Journal of Aircraft*, Vol. 19, Sept. 1982, pp. 792, 793.

[5]Kroo, I. M., "A General Approach to Multiple Lifting Surface Design and Analysis," AIAA Paper 84-2507, 1984.

[6]Kendall, E. R., "The Minimum Induced Drag, Longitudinal Trim and Static Longitudinal Stability of Two-Surface and Three-Surface Airplanes,", AIAA Paper 84-2164, 1984.

[7]Kendall, E. R., "The Aerodynamics of Three-Surface Airplanes," AIAA Paper 84-2508, 1984.

[8]Kendall, E. R., "The Theoretical Minimum Induced Drag of Three-Surface Airplanes in Trim," *Journal of Aircraft*, Vol. 22, Oct. 1985, pp. 847–854.

[9]Selberg, B. P. and Rokhsaz, K., "Aerodynamic Tradeoff Study of Conventional, Canard and Tri-Surface Aircraft Systems," *Journal of Aircraft*, Vol. 23, Oct. 1986, pp. 768–774.

[10]Feistel, T. W., Corsiglia, V. R., and Levin, D. B., "Wind-Tunnel Measurements of Wing Canard Interference and a Comparison with Various Theories," SAE Paper 810575, 1981.

[11]Williams, L. J., Johnson, J. L. Jr., and Yip, L. P., "Some Aerodynamic Considerations for Advanced Aircraft Configurations," AIAA Paper 84-0562, 1984.

[12]Ostowari, C. and Naik, D., "Post Stall Studies of Untwisted Varying Aspect Ratio Blades with an NACA 4415 Airfoil Section – Part I," *Wind Engineering*, Vol. 8, No. 3, 1984, pp. 176–194.

[13]Pope, A. and Harper, J. J., *Low-Speed Wind Tunnel Testing,* Wiley, New York, 1966.

[14]Anderson, J. D. Jr., *Introduction to Flight*, 2nd ed., McGraw-Hill, New York, 1985, pp. 351–370.